# Thermal Stability of Microstrucuture and Microhardness in Nanostructured Ni-Cr Alloy Foils Prepared by RF Sputtering Method†

MORI Masakazu*, SHIBAYANAGI Toshiya**, MAEDA Masakatsu**and NAKA Masaaki**

**Abstract**

*Nanostructured Ni-Cr binary alloy foils were fabricated by utilizing the RF-magnetron sputtering method and characterization of the foils was performed to examine microstructure, mechanical properties and thermal stability. Each foil was a nanostructured solid solution with an average grain size less than 60 nm. Average grain size increased with an increase in Cr content up to 40at%. The microhardness of the foils increased with the solute content up to 5at% and showed the maximum value of 7.0GPa, but then decreased for the further increase of Cr content. The Ni-15at%Cr alloy foil showed no decrease of microhardness up to 773K during isochronal annealing for 7.2ks, but a drastic decrease occurred as the annealing temperature was raised above 773K and the hardness decreased to 2.5GPa at 923K. Abnormal grain growth was observed in the Ni-15at%Cr alloy during isothermal annealing at 973K. The decrease of the microhardness was due to the grain growth during the annealing.*

**KEY WORDS:** (nanostructured)(microhardness)(RF sputtering)(Ni-Cr alloys)(thermal stability)

## 1. Introduction

Mechanical properties of metallic materials are strongly affected by microstructure such as mean grain size, texture, and grain boundary character distribution and so on. In particular the mean grain size is well known as a major factor affecting the mechanical properties of polycrystalline materials, and the grain size dependence of yield stress is known as "Hall-Petch relation", which is an important guideline frequently utilized for the design of microstructure. Based on this relationship high strength materials have been fabricated so far, and recently the concept is being applied to the development of ultra-fine grained materials called "nano-crystalline materials" with the grain sizes less than 100nm.

Nano-materials also have the grain size dependence explained above, and, in addition, the volume fraction of grain boundary region becomes more effective in enhancing physical, chemical and mechanical properties of grain boundary structures as the volume fraction increases. Recently development of new processes has been utilizing the distinctive characteristics of nanomaterials. For example, improvement of magnetic property has been realized by a development of nanomaterials utilizing crystallization from the amorphous state[6]. Moreover, superplasticity has also been reported in nano-Cu at room temperature with an elongation of about 1000%[7], and this unique deformation mode is attracting much attention as a promising way to increase in deformability of hard materials such as ceramics.

Therefore development of nanostructured materials has a high potential for creating novel materials having unique and excellent properties. However details and essential properties of the nanomaterials have not yet been elucidated perfectly so far, and in particular the thermal stability of microstructures should be understood systematically since so many industrial materials are alloys.

The present study aims to clarify characteristics of microstructure, mechanical properties and the thermal stability of nanostructured Ni-Cr alloy foils in order to develop novel materials based on the control of microstructure at the nano-level. Ni-Cr alloys are suitable for investigating the effects of solute content on microstructures because of the large solubility of Cr[8].

Received on May 31, 2002

* Graduate Student
** Associate Professor
*** Research Associate
**** Professor

Transactions of JWRI is published by Joining and Welding Research Institute of Osaka University, Ibaraki, Osaka 567-0047, Japan

## 2. Experimental procedure

### 2.1 Fabrication of Ni-Cr alloy foils

Magnetron RF sputtering method (ANELVA Co.Ltd., type SPF-210H) was utilized to produce nanostructured Ni-Cr alloy thin foils ranging 10 to 20μm in thickness using a pure Cr (99.9mass%) target and pure Ni (99.7mass%) pieces placed on it to change composition. The base pressure was below 2.0 x $10^{-6}$ Pa, and the Ar gas pressure for sputtering was 0.8Pa. Substrates were square plates 20mm and 1mm in thickness made of pure Cu. Distance between the substrate and the target was 350mm. Details of the sputtering condition are summarized in **Table 1**.

### 2.2 Evaluation of Ni-Cr alloy foils

Microstructural evaluation was performed using X-ray diffraction (Mac Science Co.Ltd., type M03XHF2), EPMA(JEOL Co.Ltd., JXA-8600) and TEM (JEOL Co.Ltd., JEOL-1200) techniques. X-ray diffraction(XRD) patterns were obtained by the $\theta$-$2\theta$ method using Cu-Kα line(40mA, 40kV). Composition of the deposited foils was the average value of 7 points after eliminating both minimum and maximum values from 9 measured points on the foil. Specimens for TEM observation were finally prepared by an ion milling method. The average grain size was calculated by means of the linear intercept method.

Microhardness was measured at room temperature on a cross section of foil with a Vickers testing machine (Akashi Co.Ltd., type MVK-H1). The conditions of the hardness testing were 0.245N loading pressure and 25s holding time.

Thermal stability of microstructure and microhardness of each foil was estimated by isochronal annealing for 7.2ks and isothermal annealing at temperatures ranging from 773K to 973K. Specimens for the annealing were sealed in a evacuated quartz capsule, followed by the heat treatment in a muffle furnace.

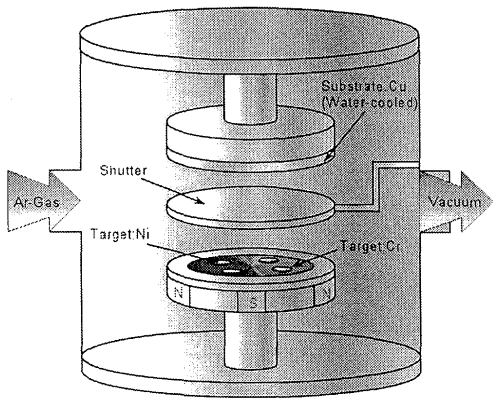


**Fig.1** Schematics of the apparatus for magnetron RF sputtering.

**Table 1** RF magnetron sputtering conditions for the foil preparation.

| | |
|---|---|
| Vacuum (Pa) | $2.0\times10^{-5}$ |
| Ar-Gas pressure (Pa) | 8.0 |
| Sputtering power (W) | 50 |
| Sputtering time (s) | 180 |
| Discharge current (mA) | 120 |
| Voltage of anode target (V) | 1.7 |

## 3. Results and Discussion

### 3.1 Microstructure of Ni-Cr alloy foils deposited

**Figure 2** shows X-ray diffraction patterns of the Ni-Cr alloy foils deposited. Each foil has the thickness of about 20μm and was suitable for the usual measurement by means of $\theta$-$2\theta$method. The diffraction peaks in the figure correspond to crystalline structures, suggesting that no amorphous phase was existing in each alloy foil fabricated in the present study.

Ni-15at%Cr and Ni-55at%Cr alloy foils show a strong peak at $2\theta$=45 and a weak peak at $2\theta$=95 degrees. These peaks correspond to FCC structure and each peak is (111) and (222) planes, respectively. Since the peak position shifted to a lower angle as the Cr content increased, solution of Cr yielded an increase of the lattice parameter. In addition, these deposited foils possess strong orientation on the normal direction of the foil plane.

Ni-78at%Cr alloy foil shows diffraction peaks at $2\theta$=39.30, 44.12 and 63.68 degrees, and these peaks were

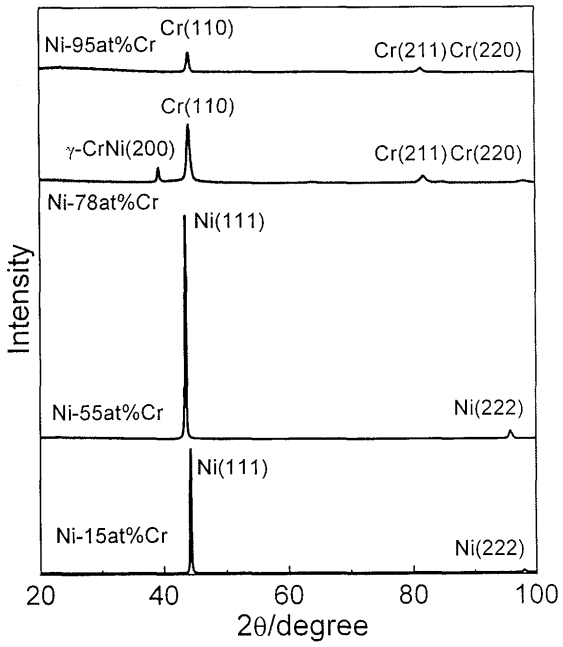


**Fig.2** XRD patterns of the Ni-Cr alloy foils deposited.

determined to correspond to (200) of γ-CrNi(cubic, a=0.455nm) phase, (211) and (220) planes of BCC Cr-base phase, respectively. Ni-95at%Cr alloy foil shows only BCC single phase with diffraction peaks at $2\theta$=44.08, 64.08 and 98.02 degrees, corresponding to (110), (210) and (220) planes, respectively.

**Figure 3** shows a phase stability diagram of the present alloy foils along with the equilibrium phase diagram of the Ni-Cr binary system. Since the maximum solid solubility of Cr in Ni is around 50at%, the present study succeeded in producing super-saturated solid solution of Ni-Cr alloy foils containing solute Cr of more than 50at%. γ-CrNi phase is a stable phase existing at temperatures lower than 863K and in the composition ranging 22 to 40at%Cr according to the binary phase diagram, but no such phase was detected in the alloy foils having the Cr content within the FCC region indicated in the upper diagram. Therefore the foils are thermodynamically unstable and precipitation of Cr-phase or γ-phase should occur when the foils are kept at elevated temperature.

Meanwhile the BCC region at the Cr rich side is within the maximum solubility of Ni, but precipitation of second phase would occur depending on the aging temperature since the solubility depends strongly on temperature. The following sections focus on Ni-Cr alloy foils with solute contents in the FCC region regarding the characterization of microstructure, mechanical properties and thermal stability of these features.

**Figure 4** shows the changes of microstructure with increasing solute content observed by means of TEM plan-view observation on deposited Ni-Cr alloy foils. (A), (B) and (C) are diffraction rings and bright field images corresponding to Ni-5at%Cr, -15at%Cr and –40at%Cr alloy foils, respectively. These images clearly show equi-axed polycrystalline microstructure, and the average grain diameter was calculated as 20nm, 45nm and 56nm for Ni-5at%Cr, -15at%Cr and -40at%Cr alloy foils, respectively. The diffraction rings indicate that the materials consist of quite fine grains, and every diffraction ring corresponds to the FCC structure. No precipitates were observed. These results are consistent with the result obtained by XRD measurements shown in Fig.2. Consequently the foils deposited are concluded to be nano-structured polycrystalline materials.

The grain size dependence of Ni content shown in Fig.4 is an opposite tendency of other reports such as the case of Cr-B and Cr-Ni alloy foils[9)-11)]. The reason could be related to specificity of the frequency of nuclei or the migration rate

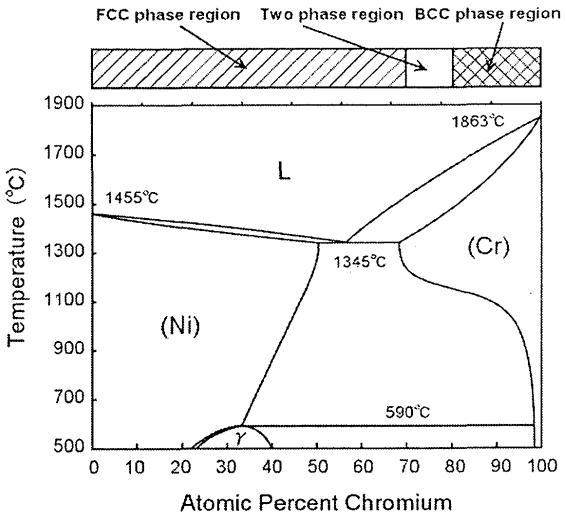


**Fig.3** Phase stability diagram of the deposits and the equi librium binary phase diagram of Ni-Cr alloy.

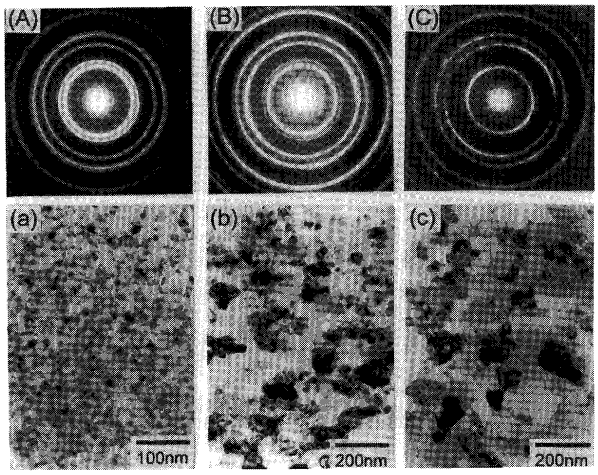


**Fig.4** TEM observations of nanocrystalline Ni-Cr alloy foils. (A) Ni-5at%Cr, (B) Ni-15at%Cr, (C) Ni-40at%Cr.

of grain boundaries in the alloy foils. The weak solute dependence of the slope of the liquids on the Ni side in the binary phase diagram would result in almost equal frequency of nucleation regardless of solute content because of the weak dependence of composition on the degree of super-cooling. Further investigations are required concerning the effect of increasing solute content on grain boundary migration and grain growth process.

### 3.2 Micro-hardness of Ni-Cr alloy foils deposited

**Figure 5** shows the effect of Cr content on microhardness of nanocrystalline Ni-Cr alloy foils. Ni-5at%Cr alloy foil has a hardness of 5.2GPa, and an increasing Cr content brings about monotonous hardening of the alloy foils up to 15at% of solute Cr. The maximum

value was 7.0GPa for Ni-15at%Cr alloy. But further addition of solute caused a slight decrease of the hardness down to 6.5 GPa for Ni-15at%Cr alloy.

Grain size dependence of micro-hardness in Ni-15at%Cr alloy foil was then investigated and the result is shown in **Fig.6**. In this case grain size was controlled by changing the power of the RF generator. Every specimen had an equi-axed grain structure. Two regions with opposite dependence of grain size on the hardness exist separated by the critical grain size of 40nm. Softening of the foil is occurring in the smaller grain size region, and this is a typical feature of nanomaterials, as has been reported.

Generally, Hall-Petch relationship has been widely applied to so many kinds of polycrystalline materials and the rule is also known to be applicable to the grain size dependence of hardness in many cases. Nano-materials, however, show a positive dependence of grain size on the mechanical properties, *i.e.* a softening behavior with decreasing grain size called "Inverse Hall-Petch relation" as shown in Fig.6. Hereafter, the mechanical properties of nano Ni-Cr alloy foils will be discussed focusing on two types of dependence such as (1) solute content and (2) grain size.

Grain size dependence should be considered in relation to the existence of mobile dislocations in such nano-grains. The least distance between two dislocations of the same sign on a glide plane should determine the minimum grain size that the Hall-Petch relation can hold. The least value is given by the following equation[12] that was derived for the case of edge dislocations:

$$l_c = \frac{3Gb}{\pi(1-\nu)\cdot H} \cdots\cdots (1)$$

where, G is shear modulus, b is Burgers vector, ν is Poisson's ratio and H is the hardness of a given material.

In order to evaluate the minimum grain size called "critical grain size" for the present alloy foils, each parameter in the equation was then measured or quoted from the literature. Elastic constant was measured utilizing a dynamic hardness test. The calculated and actual grain sizes are summarized in **Table 2**. Every specimen has a critical grain size that is smaller than the actual one, suggesting that dislocations can cause plastic deformation of these foils. In other words, the Hall-Petch rule can hold in this case.

The other estimation of the critical grain size is based on the "Orowan stress" that forces a dislocation to be moving against the pinning force caused by precipitates. The stress is applied for the punch-out of a dislocation from a grain

**Table 2** Grain sizes of nanocrystalline Ni-Cr alloy foils.

| | Grain size (nm) | $lc$(nm) |
|---|---|---|
| Ni-5at%Cr | 20 | 7.8 |
| Ni-15at%Cr | 45 | 6.9 |
| Ni-40at%Cr | 56 | 8.5 |

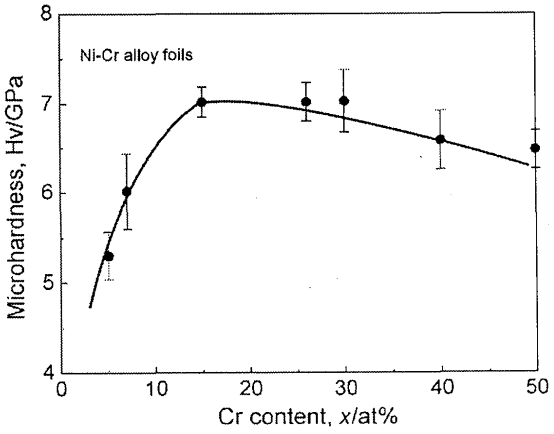


**Fig.5** Effect of Cr content on the microhardness of the nanocrytalline Ni-Cr alloy foils.

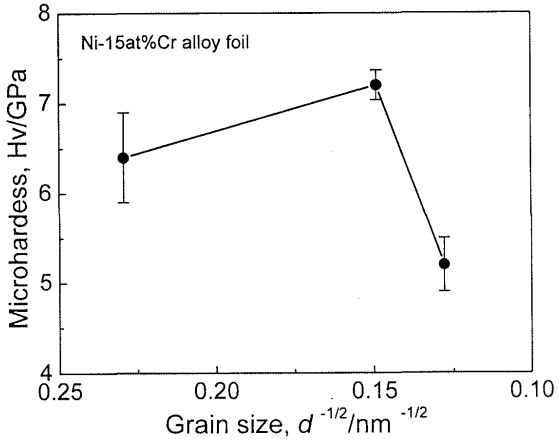


**Fig.6** Grain size dependence of microhardness in Ni-15at%Cr alloy foil.

boundary. In this case, the pinning site is a triple junction, and the length of the grain boundary is corresponding to the distance of precipitates in the Orowan model. Ni-15at%Cr alloy foil has the average grain size of 45nm, requiring the critical shear stress of at least 550MPa, This value is only8% of the actual hardness measured for the foil, suggesting that dislocations can play some important roles in the plastic deformation of the foil.

The effect of solute content on hardness in nano-structured alloy foils will be discussed in the following section based on the existence of dislocations in grains and their contribution to plastic deformation as discussed above.

As seen in Fig.5, dependence of solute content on hardness is divided into two regions: (1) Cr content less than 15at% where hardening occurs with increasing solute content, (2) Cr content more than 15at% where the opposite tendency occurs. In the latter region the hardness is affected by two mechanisms such as the softening caused by grain growth and the solution hardening mechanism. These two mechanisms are competing with each other and the actual data suggests the softening behavior is more effective in the second region.

On the other hand, the former region is also affected by the competing two mechanisms working in the softening region, and the solution hardening mechanism should be concluded to be relatively effective in this case. But this is in contrast to the explanation for the softening of the foil, since both grain size and solute content are still increasing with solute content in each region. Therefore, we should take the third factor into account in order to explain the complicated dependence of solute content on the hardness. As a possible factor affecting the mechanical properties of the present nano-materials, volume fraction of grain boundary region will be discussed in the following section.

Nanomaterials have been reported to show peculiar characteristics, strongly affected by properties of grain boundaries, that are quite different from those of conventional grain sizes larger than micron meters[5]. Assuming the width of grain boundary region as 1nm, the volume fraction of grain boundary region in the present alloy foils was estimated utilizing a formula proposed by Takaki et al[13], and the results are presented in **Table 3**. The volume fraction decreases from 17% to 6% in the first region as the grain size increases from 20 to 45nm, and is still decreasing in the second region where the value reaches 5.2% for the grain size of 56nm. This result indicates that the first region has larger reduction ratio of volume fraction per one at% than the second region. As the grain boundary region is a favorable site for both release of, and a sink for dislocations, larger volume fractions makes plastic deformation more easy. Indeed, Fe-Al alloy is reported to has nanocrystalline structure[14]. Taking into account the possess grain size dependence of hardness that deviates significantly from the Hall-Petch relation when the alloy role of the grain boundary region in the deformation process discussed so far, the hardening behavior in the first region would be explained by a reduction of the volume fraction of grain boundary region. In addition, mobile dislocations of the present nano-grain foils would affect the plastic behavior since the actual grain size of each foil exceeds the critical grain sizes as listed in Table 3. However, the volume fraction would play a dominant role in the plastic behavior of the foils.

**Table 3** Calculated volume fractions of grain boundaries in nano-structured materials with various grain sizes.

| Grain size (nm) | Volume fraction of grain boundary (%) (Grain boundary thickness = 1nm) |
|---|---|
| 20 | 17.4 |
| 45 | 6.4 |
| 56 | 5.2 |

### 3.3 Thermal stability of microstructure in Ni-Cr alloy foils

*3.3.1 Changes of microstructure and hardness during isochronal annealing*

**Figure 7** represents the variation of microhardness of Ni-15at%Cr alloy foil after isochronal annealing for 7.2ks. The foil maintains almost the same hardness as deposited foil up to 773K. But increasing annealing temperature brings about a slight decrease at higher temperature and a drastic softening occurs when the temperatures exceeds 873K, reducing the hardness down to 2.5GPa at 923K, followed by little change above this temperature.

The effect of annealing temperature on the hardness was then investigated in detail by means of XRD measurement, and the result is shown in **Fig.8**. The foil deposited shows a (111) orientation, and this tendency still appears in the foils annealed at elevated temperature by 773K. The orientation distribution changes when the annealing temperature exceeds 973K, and some other diffraction peaks such as (200) peak increase their intensity, suggesting a scattering of orientation distribution in the foils. Each peak shows no change in diffraction angle, nor the existence

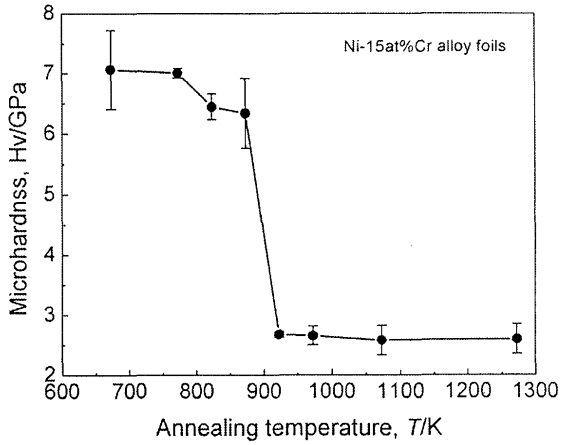


**Fig.7** Variation of microhardness of Ni-15at%Cr alloy foils isochronally annealed for 7.2ks.

present system. A similar change of the orientation was of the other peaks corresponding to second phase. This result is well consistent with the phase diagram of the observed for Ni-40at%Cr alloy foil that shows single phase at each annealing temperature.

*3.3.2 Changes of microstructure and hardness during isothermal annealing*

**Figure 9** shows variations of microhardness of Ni-15at%Cr alloy foils ishothermally annealed at 773, 873, 923 and 973K, where all the specimen are in the single phase. As a comparison, the hardness of deposited foil is also indicated with a dashed line in the figure. An abrupt decrease of hardness appears at each annealing temperature, and the critical annealing time for the big drop shifted to longer times with decreasing annealing temperature. This temperature dependence means that a thermally activated process controls the phenomenon occurring at elevated temperature.

Detailed analyses for the evolution of microstructure in the annealed foils were then performed utilizing XRD measurement and TEM observation. **Figure 10** represents XRD patterns of Ni-15at%Cr alloy foils after isothermal annealing at 973K. A strong peak corresponding to (111) plane was observed for the specimens annealed until $10^2$s. On the other hand, the other peaks such as (200) reflection increased their intensity as the annealing proceeded, and (200) and (311) reflections came to be observed clearly after $10^4$s.

**Figure 11** shows diffraction patterns and bright field images taken by the TEM method on Ni-15at%Cr alloy foils isothermally annealed at 973K for (A) $10^2$s, (B) $10^3$s and (C) $10^4$s. The foil annealed for $10^2$s shows equi-axed structure with the average grain size of 52nm, but the annealing for $10^3$s yielded mixtures of anomalously coarse and small grains as clearly shown in (B). Grain sizes of coarse and small grains were 72nm and 1003nm, respectively. In this regard, a spotty diffraction pattern tended to appear among the ring like patterns. Normal directions of these coarse grains were analyzed to be different from <111>, which is consistent with the scattering of orientation observed in XRD patterns of Fig.10. Further annealing resulted in a microstructure composed only of coarse grains with the average grain size of 1049nm as shown in (C). Thus abnormal grain growth is considered to cause the softening of foils during annealing observed in Fig.9.

The grain growth process is driven by a successive

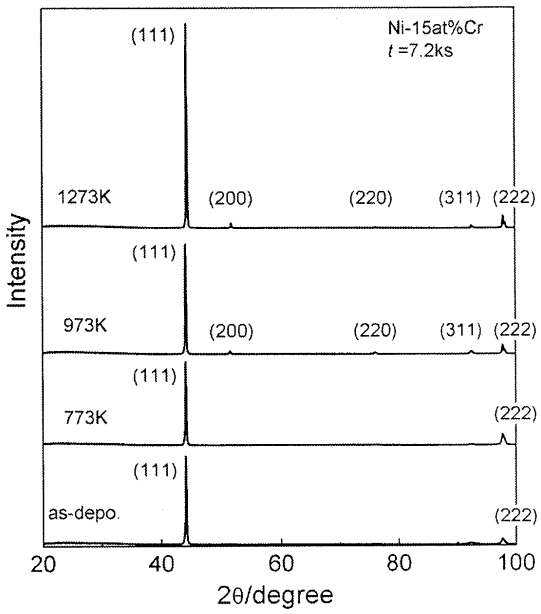


**Fig.8** XRD patterns of Ni-15at%Cr alloy foils after isochronal annealing for 7.2ks.

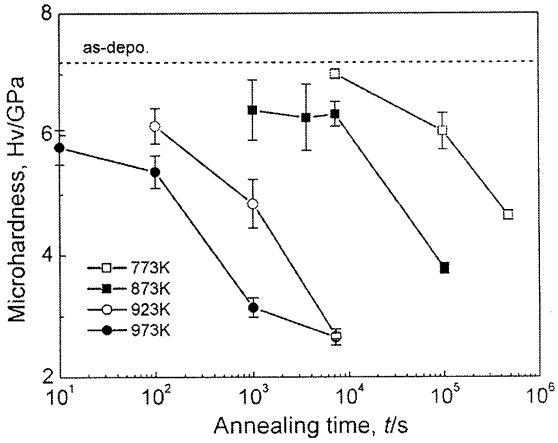


**Fig.9** Variation of microhardness of Ni-15at%Cr alloy foils isothermally annealed at various temperatures.

occurrence of grain boundary migrations. The migration behavior of boundaries is a complicated function of the structures of grain boundary and triple junctions as well as local distribution of grain size around each triple junction[15]. Abnormal grain growth appears when particular grains satisfy some special conditions for a preferential migration of boundaries around the grains. And the local conditions for the preferential migration are related to the grain boundary structure that affects the migration rate. The following section deals with abnormal grain growth observed in the present study regarding the role of local microstructure in the grain boundary migration.

There are two types of grain growth process for Nano-materials: normal grain growth and abnormal one. The

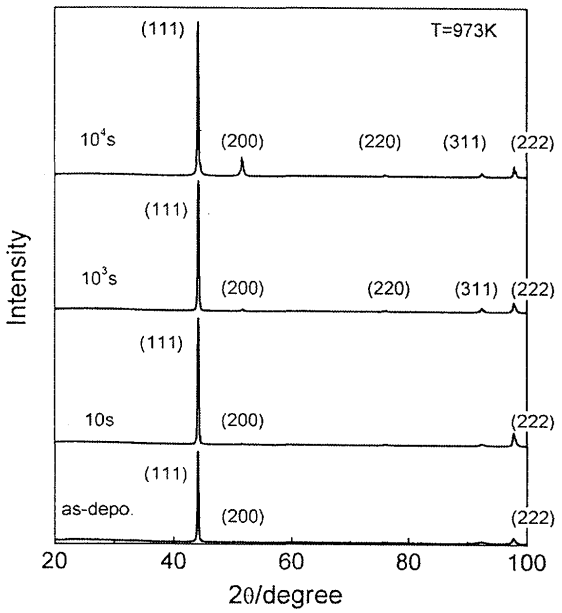


**Fig.10** XRD patterns of Ni-15at%Cr alloy foils after isothermal annealing at 973K.

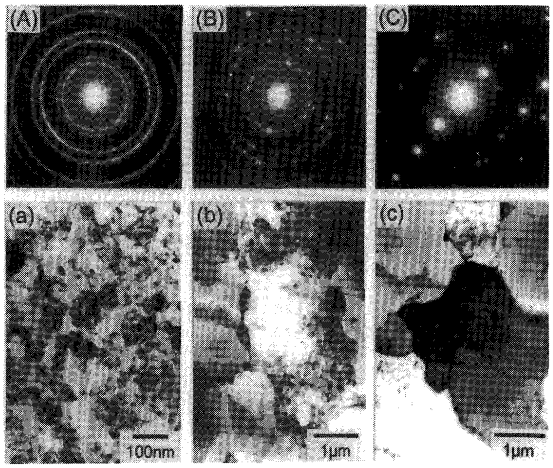


**Fig.11** TEM observations of Ni-15at%Cr alloy foils after isothermal annealing at 973K.
(A)$10^2$s, (B)$10^3$s, (C) $10^4$s.

former type has been reported for Ag[16] and mechanically alloyed NiAl intermetallics[17], and the latter type was observed in Cu[18], Ni[19] and Ag[20]. Time exponents of the equation describing grain growth in nanocrystalline Ag and NiAl were reported to be 3 and 5, respectively. The time exponents are known to be 2 for single phases, 3 for structure containing particles as dispersions, and 4 or 3 for duplex structures. Increase of the time exponent means that the migration rate of grain boundaries is reduced. Large values of the time exponent in nanomaterials of single phase suggest that grain growth proceeds based on a different type of migration behavior from materials with conventional grain size. Further investigations will need to focus on the details of migration behavior and local microstructural distributions of triple junctions, grain boundary characters, grain size and texture.

Abnormal grain growth in nanomaterials is reported to take place by three factors such as: (1) grain size distribution, (2) pinning effect caused by particles such as precipitates and oxides, (3) sub-grain coalescence[18-21]. Difference in grain sizes of neighboring grains causes a preferential growth of larger grains consuming surrounding small grains, which is known as the "size effect". This effect is essentially the same as the sub-grain coalescence. Pinning effect enhances the difference of migration rate depending on structure of each grain boundary, and this effect is also brought about by the segregation of solute atoms at grain boundaries.

The present nanostructured Ni-Cr alloy foils contain no particles as shown in the TEM micrographs. So the pinning effect does not work in the anomalous grain growth observed in Ni-15at%Cr alloy foil annealed. XRD measurement revealed the strong texture of (111) component in deposited foils while a freedom of rotation around ND//<111> axis still remains. In other words, there are large angle boundaries along with small angle boundaries or sub-boundaries in the foils. Grain boundary character distribution consist of many kinds of grain boundary structures and may yield a wide variety of energy balances at triple junctions. In this case, apart from the sub-grain coalescence model, preferential growths of some particular grains can proceed if these grains possess active triple junctions where the energy balance is not satisfied. Meanwhile, triple junctions in nanomaterials are lying in quite small distances, and their interference would affect the migration behavior of boundaries and/or triple junctions themselves. This interference effect is typical in nanomaterials and grain boundaries play a different role in the evaluation of microstructure from that in materials with micron-size grains.

Finally, the alteration of texture from a single orientation component of (111) type to a mixture type will be discussed. It is well known that Goss orientated grains in a Si-steel grow preferentially resulting in a texture change[22]. This peculiar phenomenon requires a special microstructural condition: fast growing grains are always surrounded by fast moving boundaries such as Σ5 or Σ9 coincidence boundaries. Ni-Cr alloy foils of the present study can not yield newly orientated grains by nucleation during grain growth process as long as grain rotation[23] hardly takes

place. Therefore it would be possible that non-(111) grains such as (200) component with quite small fraction satisfied the preferential growth conditions and grew anomalously by consuming (111) oriented grains that were main texture component in the deposited foils. At the same time, (111) grains could grow relatively faster than the other (111) grains if these grains contain fast moving boundaries such as high angle boundaries, and this microstructural condition is also a key factor for the abnormal growth of particular (111) grains observed in Ni-15at%Cr alloy foils.

## 4. Conclusion

The RF sputtering method was utilized for the fabrication of nanostructured Ni-Cr alloy foils, and the characterization of the foils were performed focusing on microstructure, mechanical properties and thermal stability. The following results were obtained.

The Ni-Cr alloy foils prepared by RF sputtering consisted of FCC single phase for the alloy with solute content up to 70at%, Cr+γ-phase for 70 to 80at% and BCC single phase for over 80at%.

1. Increasing solute content was observed to have a effect of increasing grain size in the as-deposited state, the average grain sizes of Ni-5at%Cr, 15at%Cr and 40at%Cr alloy foils were 20, 45 and 56nm, respectively.
2. Micro-hardness of the deposited foils increased depending on the solute content up to 15at% showing the maximum value of 7.0GPa. Further increase in the Ni content brought about the softening of the foil, and finally the hardness fell to 6.5GPa for the Ni-50at%Cr alloy foil.
3. Micro-hardness at room temperature of Ni-15at%Cr alloy foil increased with grain refinement down to 45nm, but further refinement brought about a decrease of the hardness.
4. Nanocrystalline Ni-15at%Cr alloy foil showed an abnormal grain growth, and the coarsening resulted in the softening of the foil.

## ACKNOWLEDGEMENT

The present work was partly supported by the Ministry of Education, Culture, Sports, Science and Technology (No.13450295).

## REFERENCES

(1) N.J. Petch: J. Iron Steel Inst., **174**, (1953), 25-28.
(2) R.Birringer, H. Gleiter, H. –P. Klein and P. Marquardt: Phys. Letters, **102A**, (1984), 365-369.
(3) K. Lu, W.D. Wei and J.T. Wang: Scripta Metall., **24**, (1990), 2319-2323.
(4) A.H. Chokshi, A. Rosen, J. Karch and H. Gleiter: Scripta Metall., **23**, (1989), 1679-1683.
(5) J. Karch, R.Birringer and H. Gleiter: Nature, **330**, (1987), 556-558.
(6) K.Yoshizawa and K.Yamauchi: Bull. Japan Inst. Metals, **28**, (1989), 301-303.
(7) L.Lu, M.L.Sui and K.Lu: Science, **287**, (2000), 1466-1468.
(8) *Binary Alloy Phase Diagrams*, ed. by T. B. Massalski, ASM Intl. Metals.
(9) M.Mori, T. Shibayanagi, M. Maeda and M. Naka : Scripta Mater., **44**, (2001), 2035-2038.
(10) M.Mori, T.Shibayanagi, M.Maeda and M.Naka : Trans. JWRI, **29**, (2000), 34-35.
(11) K.Kita, H.Sasaki, J.Nagahora and A. Inoue: J. Powder and Powder Metall. **47**, (2000), 406-411.
(12) G.Palumbo, S.J. Thorpe, and K.T. Aust: Scripta Metall. **4**, (1990), 1347-1350.
(13) M.A.Morris-Munoz, A.Dogde and D.G.Morris : NanoStructured Mater., **11**, (1999), 873-885.
(14) T. Shibayanagi, M. Maeda and M. Naka : J. High Temp. Soc., **26**, (2000), 28-35.
(15) R. Dannenberg, E.Stach, J.R. Groza, B.J. Dresser : Thin Solid Films, **379**, (2000), 133-138.
(16) L.Z. Zhou and J.T.Guo, Scripta Mter., **40**, (1999), 139-144.
(17) V.Y. Gertsman and R. Birringer : Scripta Mater., **30**, (1994),577-581.
(18) U.Klement, U. Erb, A.M. El-Sherik and K.T. Aust : Mater. Sci. and Eng. **A203**, (1995), 177-186.
(19) R. Dannenberg, E.A. Stach, J.R. Groza, B.J. Dresser: Thin Solid Films, **370**, (2000), 54-62.
(20) N.Wang, Z.Wang, K.T. Aust and U.Erb: Acta Mater., **45**, (1997),1655-1669.
(21) C.G.Dunn: Acta Metall., **2**, (1954), 173-183.
(22) T.Shibayanagi, K.Sumimoto and Y.Umakoshi: Scripta Mater., **34**, (1996), 1491-1495.
(23) Y.Kimura, S.Takaki, S.Suejima, R.Umemori, and H.Tamehiro : ISIJ Intl., **39**, (1999), 176-182.